Electro-optic measurement of terahertz pulse energy distribution

J. H. Sun, $^{1,2,3,a)}$ J. G. Gallacher, 2 G. J. H. Brussaard, 4 N. Lemos, 5 R. Issac, 2 Z. X. Huang, 3 J. M. Dias, 5 and D. A. Jaroszynski $^{2,b)}$

(Received 27 April 2009; accepted 14 September 2009; published online 5 November 2009)

An accurate and direct measurement of the energy distribution of a low repetition rate terahertz electromagnetic pulse is challenging because of the lack of sensitive detectors in this spectral range. In this paper, we show how the total energy and energy density distribution of a terahertz electromagnetic pulse can be determined by directly measuring the absolute electric field amplitude and beam energy density distribution using electro-optic detection. This method has potential use as a routine method of measuring the energy density of terahertz pulses that could be applied to evaluating future high power terahertz sources, terahertz imaging, and spatially and temporarily resolved pump-probe experiments. © 2009 American Institute of Physics. [doi:10.1063/1.3245342]

I. INTRODUCTION

The application of broad bandwidth terahertz electromagnetic pulses produced using femtosecond lasers have become increasingly important in areas such as biomedicine, ^{1,2} industry, ³ communications, ^{4,5} security, ^{6,7} military, ^{8,9} etc. However, measuring the energy of low repetition rate or single terahertz pulses is still a challenge. Single-shot, broadbandwidth energy detectors are not capable of measuring the energy density distribution or even the total energy of a single, picosecond duration, nanoJoule pulse. 10-12 While Jamison et al. 12-14 demonstrate the measurement of the spectrum and temporal profile of a single terahertz pulse using electro-optic detection with a chirped near infrared pulses, measuring the *energy* of a single picosecond, nanojoule pulse still remains an outstanding challenge. Here, we demonstrate a novel technique that utilizes the same electro-optic crystal for measuring both the spectrum/temporal profile and the beam profile, in order to calibrate the measurements and determine the total energy of a pulse.

II. EXPERIMENTAL SETUP

The experimental layout for determining the electric field strength is shown in Fig. 1(a). A 5 mJ pulse from a 800 nm, 50 fs Ti:sapphire laser system operating at repetition rate of 10 Hz provides both the carrier excitation for terahertz generation, and a synchronized sampling beam for electro-optic detection of the terahertz radiation. The terahertz emitter is a 50 mm diameter, 200 μ m thick, GaAs wafer that has a transverse bias field of $E_{\rm bias}$ =4 kV cm⁻¹ applied across its

surface by electrodes separated by 4 cm. A 500 fs terahertz pulse is emitted following photoexcitation of carriers on the surface of the GaAs wafer, as described by Jamison $et~al.^{13}$ The terahertz pulse is focused onto a 200 μ m thick, 10 mm diameter ZnTe (110) crystal by a 100 mm focal length, gold coated off-axis parabolic (OAP) mirror. A probe beam is picked off by a 10% beam splitter (BS). A grating stretcher, consisting of a pair of gold, blazed gratings (G1, G2), with line densities of 600/mm. The gratings are separated by 5 cm (perpendicular distance). The stretched probe beam is combined with the terahertz pulse using an indium tin oxide dichroic BS and then focused onto the ZnTe using the OAP.

The electric field strength of the terahertz pulse is determined by measuring electro-optic polarization rotation in the ZnTe crystal. ^{10,11,14,15} The probe beam is *p*-polarized, which is perpendicular to the polarization direction of the terahertz pulse. A quarter wave-plate (QWP), a half wave-plate (HWP), and a polarizer cube (analyzer) are used in combination with a spectrometer (Spectrometer) to measure the polarization rotation as a function of wavelength. This is correlated with the time evolution of the terahertz pulse amplitude through the chirp rate of the probe pulse (5 nm/ps), which is determined by the geometry of the stretcher. This effectively produces a wavelength-to-time transformation of the spectrally encoded probe pulse. ¹²

 L_1 is a 50 mm focal length lens which focuses the probe beam onto the entrance slit of the spectrometer. M_1-M_3 are 3 in. diameter dielectric mirrors and M_4-M_{13} are 1 in. silvercoated mirrors. M_9 and M_{10} are mounted on a translation stage to provide an adjustable delay between probe and terahertz pulses.

Figure 1(b) shows the experimental setup used to determine the energy density distribution. The terahertz radiation is produced, as shown in Fig. 1(a). The probe beam is again

National Electromagnetic Scattering Laboratory, Beijing 100854, People's Republic of China

²Department of Physics, University of Strathclyde, Glasgow G4 0NG, United Kingdom

³School of Information Engineering, Communication University of China, Beijing 100024, People's Republic of China

People's Republic of China

⁴Department of Applied Physics, Eindhoven University of Technology, 5600 MB Eindhoven, The Netherlands

⁵GoLP, Instituto de Plasmas e Fusão Nuclear, Instituto Superior Técnico, Av. Rovisco Pais,

1049-001 Lisbon, Portugal

a) Electronic mail: jinhaisun@gmail.com. Tel.: +86 (0) 134 3669 2716.

b)Electronic mail: d.a.jaroszynski@strath.ac.uk. Tel.: +44 (0)141 548 3057. FAX: +44 (0)141 552 2891.

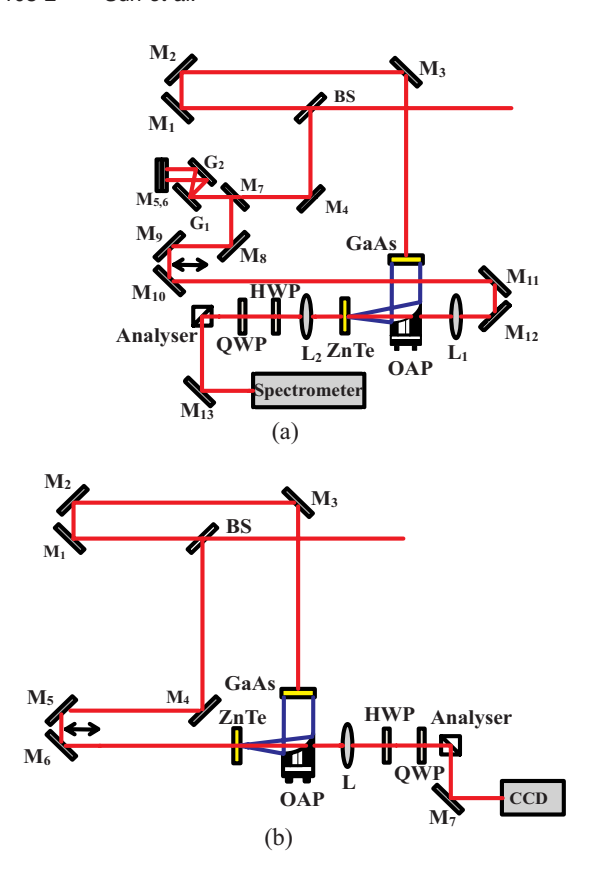


FIG. 1. (Color online) Experimental setups for measurements of the electric field strength (a) and spot energy density distribution (b).

picked off by the 10% BS and used uncompressed and collimated (unfocused) to illuminate the entire ZnTe crystal. The transmitted probe beam is imaged onto a charge coupled device (CCD) camera using a 500 mm focal length lens. Electro-optic induced polarization rotation is measured using QWP, HWP, and the polarizer cube (analyzer). M_5 and M_6 , mounted on a translation stage, provide an adjustable delay as above.

III. MEASUREMENT AND ANALYSIS

A. Terahertz electric field measurement

To minimize the transmission of the probe in the absence of the terahertz pulse, the QWP and the ZnTe crystal are initially removed. The HWP is then rotated to minimize the signal on the spectrometer. In this geometry, the probe beam after the HWP is s-polarized and is therefore rejected by the polarizer cube [analyzer in Fig. 1(a)]. With the HWP set, the QWP is inserted and, again, the signal is minimized. This ensures that the probe beam is linearly polarized at that specific setting of the QWP. The ZnTe crystal is then inserted and the spectrum was measured using the spectrometer to ensure that it does not change. This also ensures that no measurable residual birefringence from the crystal exists at that angle. The crystal is inserted with its crystal axes at approximately 45° to the polarization plane of the probe (the angle is later tweaked to optimize the signal-to-noise ratio in the final measurement).

The absolute electric field amplitude of the terahertz pulse is determined by setting the QWP to 45° (i.e., to pro-

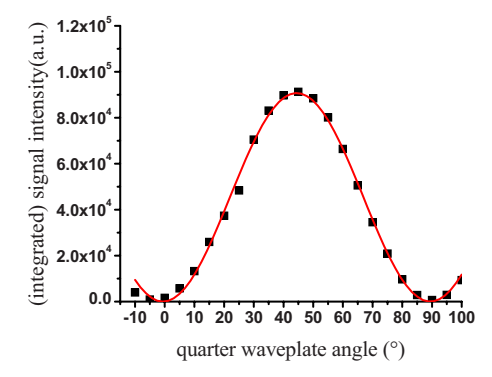


FIG. 2. (Color online) Transmitted probe beam intensity measured as a function of the QWP angle. The solid line is a fit to $I_{\text{max}} \sin(x-x_0)$.

duce circular polarized light). To accurately determine this angle, the transmission for different angles of the QWP (without the presence of terahertz) is measured, as shown in Fig. 2. Maximum transmission occurs at 45° , and thus the transmitted intensity, I_T , is given by

$$I_T^{\text{(THz=0)}} = \frac{1}{2}I_0T,\tag{1}$$

where I_0 is the intensity of the incoming probe beam, and T is the transmission coefficient of the crystal and the other optical components (due to reflections at surfaces).

With the terahertz present, the transmitted intensity of the laser is given by 16

$$I_T^{\text{(THz}\neq0)} = \frac{1}{2} (1 - \cos \Gamma_{\text{THz}} \cos^2 2\delta + \sin \Gamma_{\text{THz}} \sin 2\delta) I_0 T,$$
(2)

where δ is the rotation angle of the QWP and the phase retardation is given by

$$\Gamma_{\text{THz}} = \frac{2\pi}{\lambda_0} L n^3 r_{41} E_{\text{THz}},\tag{3}$$

where λ_0 is the laser central wavelength, L is the thickness of the ZnTe crystal, n is its refractive index at 800 nm (2.85), r_{41} is the electro-optic coefficient of the crystal in this configuration (4.0×10⁻¹² m/V), and $E_{\rm THz}$ is the terahertz electric field strength in the crystal. With the QWP set at 45° (i.e., producing a circularly polarized probe beam), we can measure the effect of the terahertz pulse on the transmitted probe laser signal, and Eq. (2) reduces to

$$I_T^{(\text{THz}\neq 0)} = \frac{1}{2}(1 + \sin \Gamma_{\text{THz}})I_0T.$$
 (4)

The spectra of the stretched probe beam with and without the terahertz present are shown in Fig. 3. By combining Eqs. (1) and (4), we have

$$\Gamma_{\text{THz}} = \arcsin\left(\frac{I_T^{(\text{THz}\neq 0)}}{I_T^{(\text{THz}=0)}} - 1\right). \tag{5}$$

To calculate the terahertz field outside the crystal, we need to correct for the reduction in the transmitted field amplitude due to reflection at the surface [i.e., $t_{\rm THz} = 2/(1 + n_{\rm THz}) = 0.5$, where $n_{\rm THz} \approx 3$]. The electric field strength of the terahertz pulse is thus given by

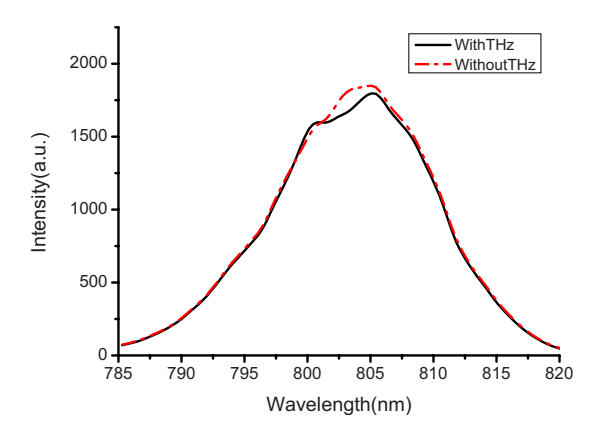


FIG. 3. (Color online) Spectra of the probe laser with and without the terahertz pulse. The QWP is set at 45° (circularly polarized probe beam).

$$E_{\rm THz} = \frac{\Gamma_{\rm THz} \lambda_0}{2 \pi L n^3 r_{41}} \cdot 2 = \frac{\lambda_0}{\pi L n^3 r_{41}} \arcsin \left(\frac{I_T^{(\rm THz \neq 0)}}{I_T^{(\rm THz = 0)}} - 1 \right). \quad (6)$$

The resulting terahertz field strength is shown in Fig. 4.

B. Terahertz energy density measurement

The terahertz pulse energy density distribution is measured by placing the ZnTe crystal at the focal position and configuring the probe beam to be collimated and (in this setup) counterpropagating, as shown in Fig. 1(b). The QWP is rotated to 2–3° for an optimum signal-to-background ratio (i.e., near linear polarization). The probe beam is fully compressed (50 fs). The crystal is then imaged onto a CCD camera. The magnification of the imaging system is determined using a 200 µm diameter wire. This gives a calibration factor of 5 µm/pixel. The energy density distribution of the terahertz beam is measured by subtracting the image without the terahertz signal present (the background) from the image with the terahertz beam present. The result is shown in Fig. 5. To improve signal-to-noise ratio, we have averaged over ten images. Because the transmitted signal is nearly linearly polarized, the transmitted intensity is given by

$$\frac{I_T}{I_0 T} = \frac{1}{2} (1 - \cos \Gamma_{\text{THz}}) = \sin^2 \frac{\Gamma_{\text{THz}}}{2} \approx \frac{\Gamma_{\text{THz}}^2}{4},\tag{7}$$

with Γ_{THz} given by Eq. (3). Equation (7) shows that the measured transmitted intensity of the probe laser beam in this configuration is proportional to the intensity of the terahertz pulse. The energy density distribution of the terahertz

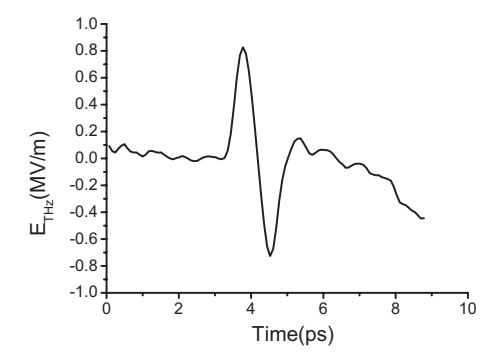


FIG. 4. E_{THz} measured as a function of time, where t=0 is arbitrary.

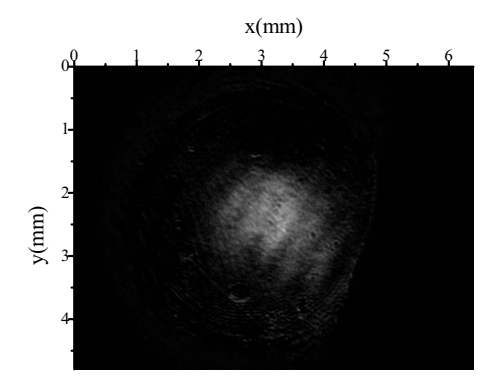


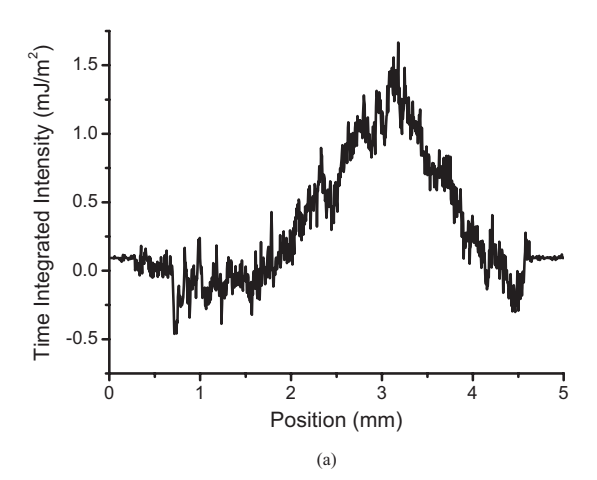
FIG. 5. Terahertz focal spot.

pulse can now be calculated by numerically integrating (the square of) the signal of Fig. 4

$$u_{\rm THz} = \varepsilon_0 c \int_t E_{\rm THz}^2 dt. \tag{8}$$

The horizontal and vertical line-outs of the spot are shown in Fig. 6.

The total energy of the terahertz pulse is found by integrating over both the area of terahertz focal spot (Fig. 5) and the duration of the terahertz pulse (Fig. 4)



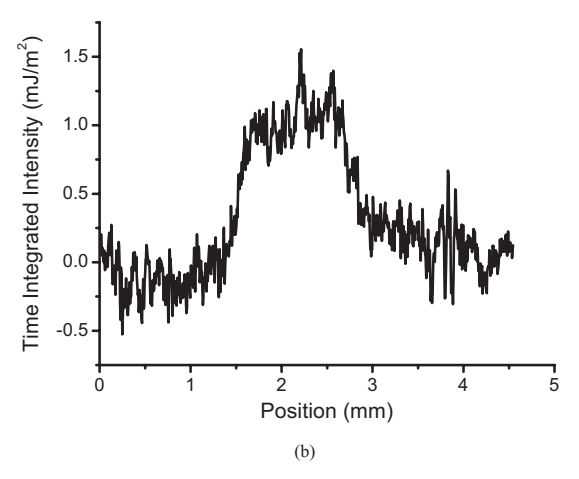


FIG. 6. Horizontal (a) and vertical (b) line-outs of the terahertz focal spot energy density.

$$U_{\text{THz}} = \varepsilon_0 c \iint_{A.t} E_{\text{THz}}^2 dA dt = (2.6 \pm 0.3) \times 10^{-9} \text{ J},$$
 (9)

where the error arises mainly from noise in the measurement of the terahertz focus spot.

IV. CONCLUSIONS

We have presented a method of measuring the energy density distribution of a terahertz radiation pulse using the electro-optic effect in a nonlinear crystal. This is achieved by measuring both the absolute electric field strength of the terahertz pulse and its transverse profile. The measurement of the electric field amplitude is used as a calibration to relate the measured transverse profile of the terahertz spot to the energy distribution. Provided that the duration of the terahertz pulses does not change (which can be easily checked), the measurement of the terahertz focal spot then provides a single shot measurement of both the total energy and the energy density distribution. This method could find use in the development of future high power terahertz sources and in spatially and temporarily resolved pump-probe experiments.

ACKNOWLEDGMENTS

The U.K. team acknowledges the support of the EPSRC Research Council, U.K., Grant No. EP/E001815, and the China Scholarship Council, China.

- ¹E. Berry, A. J. Fitzgerald, N. N. Zinov'ev, G. C. Walker, S. Homer-Vanniasinkam, C. D. Sudworth, R. E. Miles, J. M. Chamberlain, and M. A. Smith, Proc. SPIE **5030**, 459 (2003).
- ²N. N. Zinov'ev, A. S. Nikoghosyan, and J. M. Chamberlain, Proc. SPIE **6257**, 62570P (2006).
- ³S. Wietzke, F. Rutz, C. Jördens, N. Krumbholz, N. Vieweg, C. Jansen, R. Wilk, and M. Koch, Proc. SPIE 6840, 68400V (2007).
- ⁴R. Piesiewicz, J. Jemai, M. Koch, and T. Kurner, Proc. SPIE 5727, 166 (2005).
- ⁵N. Krumbholz, K. Gerlach, F. Rutz, M. Koch, R. Piesiewicz, T. Kürner, and D. Mittleman, Appl. Phys. Lett. 88, 202905 (2006).
- ⁶I. V. Minin and O. V. Minin, Proc. SPIE **6212**, 621210 (2006).
- ⁷ M. J. Hagmann, B. A. McBride, and Z. S. Hagmann, Proc. SPIE **5411**, 51 (2004).
- ⁸ Y. Ma, L. Yan, and J. M. Seminario, Proc. SPIE **6212**, 621204 (2006).
- ⁹N. Kislov, M. Sarehraz, and E. Stefanakos, Proc. SPIE **6542**, 65421H
- ¹⁰ X. Y. Peng, O. Willi, M. Chen, and A. Pukhov, Opt. Express 16, 12342 (2008).
- ¹¹Z. Jiang and X.-C. Zhang, Appl. Phys. Lett. 72, 1945 (1998).
- ¹² S. P. Jamison, J. Shen, A. M. MacLeod, W. A. Gillespie, and D. A. Jaroszynski, Opt. Lett. 28, 1710 (2003).
- ¹³ S. P. Jamison, B. Ersfeld, and D. A. Jaroszynski, Curr. Appl. Phys. 4, 217 (2004).
- ¹⁴ S. P. Jamison, G. Berden, A. M. MacLeod, D. A. Jaroszynski, B. Redlich, A. F. G. van der Meer, and W. A. Gillespie, Nucl. Instrum. Methods Phys. Res. A 557, 305 (2006).
- ¹⁵ J. van Tilborg, C. B. Schroeder, Cs. Tóth, C. G. R. Geddes, E. Esarey, and W. P. Leemans, Opt. Lett. 32, 313 (2007).
- ¹⁶ Q. Chen, M. Tani, Z. Jiang, and X.-C. Zhang, J. Opt. Soc. Am. B 18, 823 (2001).